DOI 10.1515/hf-2013-0011 — Holzforschung 2013; 67(8): 931–940

Daniel Van Opdenbosch, Jörg Dörrstein, Somruedee Klaithong, Tobias Kornprobst, Johann Plank, Sami Hietala and Cordt Zollfrank*

Chemistry and water-repelling properties of phenyl-incorporating wood composites

Abstract: The properties of materials are presented, which are resulting from a combined inorganic-organic modification of wood with phenyltrimethoxysilane or phenyltriethoxysilane in a simple one-step impregnation treatment. The permanent swelling of the wood showed that the precursors entered the cell walls. The inclusion of phenyl groups, manifest by nuclear magnetic resonance spectroscopy, made the resulting wood composites highly hydrophobic, as evidenced by their low wettability and antishrink efficiencies of up to 44%. Impedance spectroscopy indicated that wood methylol groups took part in the condensation reactions with hydrated siloxanes, contributing to the high hydrophobicity and making the added phase resistant to leaching. The composites exhibited high weight percentage gains of up to 52% and ash contents up to 19%. The thermal properties of precursor solutions and products were assessed by differential scanning calorimetry and thermogravimetric analysis and compared with the more common silica precursor, tetraethyl orthosilicate.

Keywords: ^{13}C CPMAS, differential thermal analysis (DTA), differential scanning calorimetry (DSC), electrical impedance spectroscopy (EIS), hydrophobic wood, phenyl, phenyltriethoxysilane (PTEOS), phenyltrimethoxysilane (PTMOS), ^{29}Si solid-state NMR, siloxane, tetraethyl orthosilicate (TEOS), thermogravimetric analysis (TGA), wood composite

***Corresponding author: Prof. Dr. Cordt Zollfrank,** Fachgebiet Biogene Polymere, Technische Universität München am Wissenschaftszentrum Straubing, Schulgasse 16, D-94315 Straubing, Germany, e-mail: cordt.zollfrank@tum.de
Daniel Van Opdenbosch and Jörg Dörrstein: Fachgebiet Biogene Polymere, Technische Universität München am Wissenschaftszentrum Straubing, Schulgasse 16, D-94315 Straubing, Germany
Somruedee Klaithong, Tobias Kornprobst and Johann Plank: Lehrstuhl für Bauchemie, Technische Universität München, Lichtenbergstraße 4, D-85747 Garching, Germany
Sami Hietala: Laboratory of Polymer Chemistry, Department of Chemistry, University of Helsinki, FIN-00014 Helsinki, Finland

Introduction

Tetraethyl orthosilicate (TEOS) is a common silica precursor for the mineralization of biological structures, such as wood and wood fibers, to improve their properties or replicate them as ceramics. Silica-treated wood has improved water-repelling properties (Donath et al. 2004). It is also more resistant to fire (Saka and Ueno 1997), microbes (Tanno et al. 1998; Mahltig et al. 2008), wood borers (Cookson et al. 2007), and UV decay (Miyafuji et al. 2004). The deposition of the treatment phase within the cell walls leads to superior properties of the resulting materials compared with a mere surface deposition (Allan et al. 1992; Donath et al. 2004; Xie et al. 2010). In its monomeric state, TEOS can penetrate into cell walls (Saka et al. 1992), whereas this is not possible for prehydrolyzed and precondensed siloxane species due to their larger molecular dimensions (Unger et al. 2012). The penetration of TEOS into cell wall pores down to a size of as low as 1 nm was recently described by means of a combined delignification and chemical functionalization approach (Van Opdenbosch et al. 2011; Fritz-Popovski et al. 2013). If the presence of water is limited to the cell wall, hydrolysis and condensation (as shown in Figure 1a and b) will mainly occur within the cell wall.

However, TEOS has a reported boiling point of 168°C (Rösch et al. 2000) and evaporates partly during the drying step that follows the impregnation. Precursors with lower vapor pressures than TEOS are therefore desirable. One way to obtain these is by substituting one of the ethoxy groups in TEOS with other functional groups. Such compounds condense to organically modified oxide-based ceramic hybrids (Jitianu et al. 2003). Due to the substituted alkyl group and its electron-donating properties, their crosslinking kinetics differ from those of TEOS. They have increased hydrolysis rates, but their condensation rates are reduced (Sanchez et al. 1996; Brunet 1998).

Compounds exhibiting higher condensation rates than alkyl-substituted TEOS are aryl-substituted ones, such as phenyltrimethoxysilane (PTMOS) and phenyltriethoxysilane (PTEOS) (Jermouni et al. 1995; Hook 1996; Sugahara et al. 1997; Kuniyoshi et al. 2006; Sun et al. 2006). They hydrolyze and condense as shown in Figure

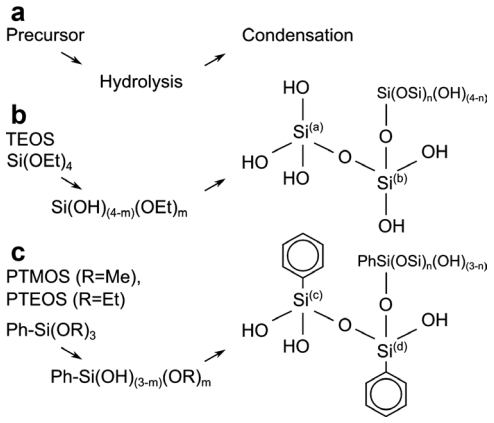

Figure 1 Principle of silicate and silane condensation (a). Formation and structures of the materials incorporated into wood cell walls after hydrolysis and partial condensation with (b) TEOS and (c) PTMOS and PTEOS. The marks on the silicon atoms refer to the nomenclature used in ^{29}Si NMR spectroscopy, that is, the bonding states: (a) Q_0^1, (b) Q_0^2, (c) T_0^1, and (d) T_0^2. Bonding to wood can occur by silyl etherification between wood hydroxyl and silanol groups under loss of water.

1c. These compounds have been characterized with regard to their surface energy and wettability when condensed into spherical particles (Wu et al. 2006) or aerogels (Rao et al. 2003). The results suggest that they have potential as hydrophobic wood-protective agents. Further, wood fibers with hydrophobic properties may show improved blending with or bonding to polymer matrices in wood-plastic composites (WPCs), where amphiphilic processing aids or silane treatments are applied when using untreated fibers (Pickering et al. 2003; Stark and Matuana 2007).

The chemical and water-repelling properties of wood treated with the organically modified alkoxide precursors PTMOS or PTEOS have not yet been extensively tested. Further, the hydroxyl groups of wood were proposed to be covalently bonded to incorporated compounds (Donath et al. 2004; Tingaut et al. 2006). It was, however, found that such reactions require elevated temperatures and high wood moisture content (Castellano and Gandini 2004). The analysis of this matter is complicated by the fact that, to date, the only method having unambiguously proven the occurrence of chemical bonds between deposited inorganic phases and wood is electrical impedance spectroscopy (EIS) (Fu and Zhao 2007).

The precursors used in the present work are tetrafunctional and trifunctional alkoxides. Their etherification is assumed to proceed via the two-step hydrolysis and condensation reaction commonly found in siloxanes (Brinker and Scherer 1990). The latter could either include two silanol groups or one silanol group and a hydroxyl group from wood. A nomenclature to describe both the hydrolysis and condensation states of the molecules is Q_m^n (quarternary) and T_m^n, respectively. They correspond to the local stoichiometries of the resulting siloxanes $SiO_{n/2}(OH)_{4-n}(OR)_m$ and $RSiO_{n/2}(OH)_{3-n}(OR)_m$. The condensed structures are purely inorganic siloxanes in the case of tetrafunctional alkoxide precursors and organic-inorganic hybrid organosiloxanes in the case of trifunctional, bifunctional, or monofunctional alkoxides, as shown in Figure 1.

The intention of the present article is to clarify the water-repelling properties and the bonding states of PTMOS and PTEOS-treated wood composites. For the characterization of these composites, the following parameters were determined: weight percentage gain (WPG), equilibrium moisture content (EMC), antishrink efficiency (ASE), and contact angle (CA). Moreover, ζ-potential measurement, nuclear magnetic resonance (NMR) spectroscopy, and EIS were applied. The thermal properties of the composites were assessed by differential scanning calorimetry (DSC) and thermogravimetric analysis combined with differential thermal analysis (TGA-DTA). The core question is whether PTMOS and PTEOS are chemically bound after their deposition in the cell walls.

Materials and methods

Chemicals were used as received: ethanol (EtOH; purity ≥98%, denaturated with 1% methylethylketone; Roth, Karlsruhe, Germany), TEOS (purity 98%; Merck, Darmstadt, Germany), PTMOS (purity 97%; Alfa Aesar, Ward Hill, MA, USA), PTEOS (purity >98%; Alfa Aesar), and cyclohexane (purity ≥99.5%; Roth).

Sample preparation

Kraft-pulped pine (*Pinus radiata*) wood fibers (KPF) with stated κ number 25 as well as EtOH-extracted ("native") and optionally sodium chlorite delignified (Van Opdenbosch et al. 2011) pine (*Pinus sylvestris*) cubes (W) of 1 cm side length were treated with PTMOS and PTEOS in EtOH solution. Untreated and TEOS-treated fibers and cubes were prepared as control samples. For 1 g wood, 1.28 g TEOS, 1.22 g PTMOS, or 1.48 g PTEOS dissolved in 10 g EtOH were used for the treatments. A 100 mbar vacuum from a membrane pump was applied to remove air and impregnate the samples. Treated samples were dried at 50°C until all visible liquid was removed and then at 75°C and 105°C for 1 day each.

Analyses

The WPGs of the impregnated samples were determined. Their EMCs were determined according to TAPPI standard T550 after storage over several days at room temperature (21°C) and an atmospheric humidity between 37% and 41%. The ash determination was performed

according to TAPPI standard T413. The dynamic surface (ζ-)potential of treated and untreated fibers were analyzed with a glass electrode (Mettler Inlab; Mettler-Toledo, Gießen, Germany on analyzer HJ83141; Hanna Instruments, Woonsocket, RI, USA) with 1 g treated wood fibers dispersed in 800 g distilled water. No pH adjustment was performed after the addition of the fibers. To eliminate the influence of wood surface inhomogeneities such as the annual growth rings, the wettabilities of the products were first determined qualitatively by preparing paper sheets on a filter paper base in a Büchner funnel connected to a 100 mbar vacuum. The time required for a 500 µl drop of deionized water (pH 6.91) to be completely absorbed into the papers to a CA of 0° was determined via video analysis. The volume and mass changes during treatment and the CA of water were determined on the wood cubes. The ASEs were determined by placing the wood cubes in distilled water at 100 mbar for 1 h and then at ambient pressure for 24 h. The wet specimens were dried at 105°C. Their wet and dry volumes, measured with a sliding caliper, served for ASE calculation (Stamm et al. 1936; Elvy et al. 1995).

Bonding states of the precursors

The leaching of precursor was assessed by aqueous Soxhlet extraction of dried and weighed KPF and subsequent drying, weighing, and ash determination. ^{13}C cross-polarization magic angle spinning (CPMAS) and ^{29}Si solid-state NMR measurements were performed at room temperature on treated wood and fibers with a Bruker Advance III spectrometer (Bruker BioSpin GmbH, Rheinstetten, Germany) operating at 500 MHz proton frequency with MAS at 10 kHz, a 4 mm rotor, a contact time of 1 ms, and 2000 collected scans with a repetition rate of 3 s. For ^{1}H decoupled ^{29}Si MAS spectra, at least 4000 scans were recorded with a repetition rate of 4 s and referenced to TMS. EIS was performed on a precision impedance analyzer (E4991A; Agilent Technologies, Santa Clara, CA, USA) with an attached materials testing fixture (A25730; Agilent Technologies) and calibrated using a polytetrafluoroethene plate with thickness of 760 µm. The fiber samples were pressed into pellets of 13 mm in diameter and their thicknesses (700–1000 µm) were determined with a micrometer screw gauge. To capture the rapid hydroxyl motions, the complex permittivity was measured at 800 exponentially increasing frequencies from 10 MHz to 1.5 GHz at an oscillation level of 100 mV (Einfeldt et al. 2001). The samples were measured in their EMC states (T 21°C, Φ 37–41%) and after heating to 105°C for 6 h and subsequent cooling to room temperature in a desiccator to eliminate the influence of adsorbed water. The results were corrected for their geometrical densities. The imaginary parts of the complex permittivities ε_r'' were plotted over the real parts ε_r' and formed sections of Cole-Cole plots (Cole and Cole 1941). The data were then fitted by Equation (1) using the scaled Levenberg-Marquardt algorithm (10^3 iterations, tolerance 10^{-4}):

$$\epsilon_r''=\epsilon_{rM}''+\sqrt{\left(\frac{\epsilon_0-\epsilon_\infty}{2}\right)^2+\left(\epsilon_r'-\epsilon_{rM}'\right)}, \quad (1)$$

where ε_{rM}'' is the Cole-Cole plot's Y-axis center, ε_{rM}' is the X-axis center, and $(\varepsilon_0-\varepsilon_\infty)/2$ is the circle radius. From the fitted parameters, the permittivities at the limiting low and high frequencies ε_0 and ε_∞ and the relaxation time distribution factor β were directly calculated from geometrical consideration of the Cole-Cole plot by Equations (2) and (3):

$$\left.\begin{matrix}\epsilon_0\\ \epsilon_\infty\end{matrix}\right\}=\epsilon_{rM}'\{\pm\}\sqrt{\left(\frac{\epsilon_0-\epsilon_\infty}{2}\right)^2-\epsilon_{rM}''^2} \quad (2)$$

$$\beta=\arccos\left(\left|\epsilon_{rM}''\right|\Big/\frac{\epsilon_0-\epsilon_\infty}{2}\right). \quad (3)$$

The generalized relaxation time τ_0 was then determined by considering the original Debye equation for the behavior of dielectrics in an alternating current field and its dispersion correction by β; see Equation (4) (Cole and Cole 1941; Kirkwood and Fuoss 1941):

$$\epsilon^*=\epsilon_\infty+\frac{\epsilon_0-\epsilon_\infty}{1+(i\omega\tau_0)^\beta}, \quad (4)$$

where ε^* is the complex dielectric permittivity and ω is the angular frequency. Asymmetric relaxation time distributions were not considered because of the measurements' confinement to the high-frequency region. To calculate τ_0, the relation between the two vectors u and v whose starting, intermediate, and end points are ε_0, a point on the Cole-Cole arc, and ε_∞ were used via Equation (5) (Cole and Cole 1941; Taylor and Aloisio 1985):

$$\log\frac{|v|}{|u|}=\beta\log(\omega\tau_0) \quad (5)$$

The vectors u and v were obtained from the fitted data and confirmed by Equation (6) (Taylor and Aloisio 1985):

$$|u+v|=\epsilon_0-\epsilon_\infty. \quad (6)$$

Thermal analyses

DSC measurements were carried out with 5 mg of the precursor solutions with a heating rate of 5°C min^{-1} (DSC12E; Mettler-Toledo). TGA and DTA were conducted on fibers placed in a combined TGA-DTA instrument (STA 409 PC TA; Netzsch Gerätebau, Selb, Germany). Details: corundum crucible, constant heating rate of 10°C min^{-1} up to 800°C under airflow.

Results and discussion

Water repellence of the composites

The ζ-potential of the untreated KPF (KPF_{untr}) (Table 1) is the half the value found for cotton in literature (Jacobasch et al. 1985), presumably owing to the residual lignin in the fibers. On the contrary, all treated fibers (KPF_{tr}; i.e., $KPF_{TEOS,\ PTMOS,\ PTEOS}$) have similar ζ-potentials of less than -60 mV at pH 5.5 and 5.9, similar to glass fibers (Jacobasch et al. 1985) and silicon dioxide in general (Attard et al. 2000). The EMC of KPF_{untr} (4.4%) is in agreement with literature (Engelund et al. 2013), whereas K_{PTMOS} and K_{PTEOS} are highly hydrophobic as shown by their low EMCs (Table 1).

Table 1 ζ-potentials and pH values of 0.125 wt% aqueous suspensions and EMCs at 37% to 41% ambient relative humidity of untreated and TEOS-, PTMOS-, and PTEOS-treated KPF.

Fiber type	ζ-potential (mV)	pH	EMC (%)
KPF_{untr}	-12	6.7	4.40
KPF_{TEOS}	-88	5.5	3.55
KPF_{PTMOS}	-63	5.8	0.87
KPF_{PTEOS}	-67	5.9	0.99

The effects of the different surface potentials on the aggregation behavior of the fibers became evident during drying. Whereas KPF_{untr} appeared as compact, cardboard-like agglomerates, the KPF_{tr} formed loose wools. In dispersion, the KPF_{tr} had equally different appearances. KPF_{untr} and KPF_{TEOS} could be shaped into sheets from a dispersion in water, whereas the KPF_{PTMOS} and KPF_{PTEOS} were not dispersible in water. Therefore, cyclohexane was used to make papers from the latter two. Water drops were completely absorbed by KPF_{untr} papers within 400 ms and by KPF_{TEOS} ones within 200 ms. The lower EMC of KPF_{TEOS} is therefore attributable to pore filling and not wettability. In the case of W_{PTMOS} and W_{PTEOS}, the water drops evaporated within 1 h without being absorbed. The CAs found on KPF_{tr} were 135° (Figure 2).

These CAs are higher than those of heat-treated wood (Pétrissans et al. 2003) and similar to those of silylated wood (Mohammed-Ziegler et al. 2008) or siloxane plasma-treated wood (Podgorski et al. 2000). Compared with reports on pine wood (W_{PTMOS}) in water or EtOH, the CAs in the present work are higher by 25% (Aaserud et al. 2009). In this work, KPF_{PTMOS} and KPF_{PTEOS} were also found to be immiscible with water and form defined emulsions. The dimensional changes in the three anatomical directions of the wood cubes (W_{tr}) and their WPGs during treatment and the ASEs of the resulting materials are compiled in Table 2.

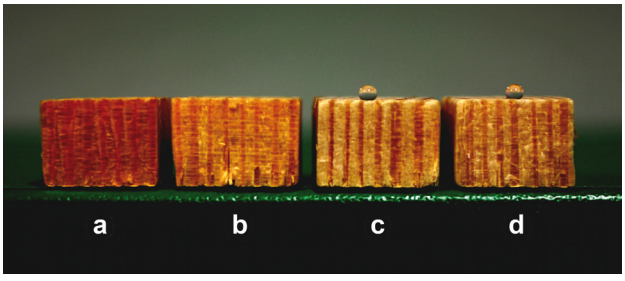

Figure 2 Drops (500 µl) of distilled water 10 min after being placed simultaneously on the radial/tangential (RT) plane of (a) untreated and (b) TEOS-, (c) PTMOS-, and (d) PTEOS-treated pine wood. PTMOS- and PTEOS-treated samples maintained a CA of 135°.

Table 2 Swelling of native (W) and delignified (W_{delig}) pine wood cubes in axial, radial, and tangential directions, their weight percent gains (WPG) after treatment with TEOS, PTMOS, and PTEOS, and the ASEs of the resulting composites.

Sample	Δl_{ax} (%)	Δl_{rad} (%)	Δl_{tan} (%)	WPG (%)	ASE (%)
W_{TEOS}	0.37	0.75	1.74	4.8	8.9
W_{PTMOS}	1.87	2.04	4.74	24.3	41.1
W_{PTEOS}	1.68	0.87	2.37	16.9	34.2
$W_{delig, TEOS}$	0.78	1.74	1.17	11.5	6.9
$W_{delig, PTMOS}$	1.18	3.77	4.73	51.1	44.8
$W_{delig, PTEOS}$	1.07	2.58	3.60	23.9	34.6

The permanent swelling of the treated wood cubes could be safely interpreted as the deposition of material in the cell walls. In axial direction, the cellulose fibrils restrict swelling. In the radial and tangential directions, the wood structure can be swollen permanently by the inclusion of the additional treatment phase in the fibril interstitials. This leads to pore filling in the cell wall, which causes increased water resistance. The observed WPG for W_{TEOS} is in agreement with literature data (Miyafuji et al. 2004; Fu and Zhao 2007), whereas the WPGs of W_{PTMOS} and W_{PTEOS} are notably higher. Delignified wood cubes W_{delig} were prepared to assess the effects of the increased cell-wall porosity also found in KPF (Fahlén et al. 2005). The differences in swelling and WPG compared with native pine match the expectations. The reduced axial swelling in W_{delig} is due to the increased swelling in radial and tangential directions and geometrical restraints (Burgert et al. 2007). The total volume changes of the treated materials ($W_{delig, tr}$) were approximately doubled by the prior delignification, indicating that the precursors penetrated the cell walls. The WPGs were also almost doubled and reached the level of KPF. The ASE values found for all W_{tr} are lower than values reported for resin- or polymer-treated wood, which themselves vary greatly (Stamm et al. 1936; Loos 1968). The data are below those of the highest ASE in acetylated wood by 40% (Rowell and Ellis 1978; Temiz et al. 2006). The ASE values were similar to those reported for wood treated with combinations of methyl methacrylate and diallyl phthalate (Rozman et al. 1995) and higher than the values reported for other substituted alkoxysilanes, which is attributable to the added incorporation of hydrophobic phenyl groups into the cell wall (Donath et al. 2004). The ASE values are also higher than those reported for wood treated with silane coupling agents (Elvy et al. 1995).

The leaching tests resulted in no detectable mass losses or changes in ash content of KPF_{PTMOS} and KPF_{PTEOS} (Table 3). For KPF_{TEOS}, a 2% mass loss and no detectable ash change was observed, indicating that the phases

Table 3 WPGs and ash contents of untreated and TEOS-, PTMOS-, and PTEOS-treated KPF.

Fiber type	WPG	Ash content (%)
KPF_{untr}	–	0.15
KPF_{TEOS}	6.9	6.2
KPF_{PTMOS}	51.9	19.4
KPF_{PTEOS}	22.2	11.9

incorporated into the cell walls were either sterically fixed or chemically bound. In the case of KPF_{PTMOS} and KPF_{PTEOS}, the low wettability of the fibers with water required the use of cyclohexane as extracting agent.

The modification routes proposed hitherto in the literature (Rowell et al. 1976) are very complex, which could be ecologically unviable after scaling up. In contrast, the modification described in the present article is a simple one-step impregnation process, in which nontoxic metal organic precursors are used with EtOH as a recyclable solvent.

Bonding states I: NMR

The ^{13}C CPMAS NMR spectrum of native pine W_{untr} (Figure 3a) is similar to published spectra (Tjeerdsma et al. 1998; Sèbe and De Jéso 2000). The removal of materials and structural changes during the treatment steps is obvious from the missing lignin OMe signal at 59 ppm in all W_{tr} with the exception of W_{TEOS} (Figure 3b). In W_{delig} (Figure 3c), and all KPF samples (Figure 3d–f), lignin was therefore effectively removed from the fibers, opening up further space for the precursors. In KPF (Figure 3d), the signal decrement at 64 and 83 ppm, ascribed to the less crystalline moiety of cellulose (i.e., C6 and C4 atoms of amorphous or paracrystalline cellulose), is indicative of its removal or mercerization (Sèbe and De Jéso 2000). In contrast to $W_{delig, TEOS}$, the hemicellulose signal at 22 ppm is missing in the KPFs (Mao et al. 2006). The spectrum of $W_{delig, TEOS}$ (Figure 3c) demonstrates the presence of residual hemicelluloses and the selectivity of the sodium chlorite delignification. A comparison with the spectrum of W_{delig} (not shown for brevity) indicates that the reduction of carbon signals typical for amorphous carbohydrates is due to their mercerization and crystallization during vacuum impregnation. The $W_{delig, TEOS}$ and W_{TEOS} show no EtOH signals at 18.1 ppm, or ethoxy groups at 57.8 ppm, indicating the complete hydrolysis of the precursor (Salon et al. 2007). The WF_{PTMOS} spectrum (Figure 3e) shows an additional weak signal at 52 ppm, which is attributed to a silicon-bonded methoxy carbon (Brindle et al. 1995). This indicates, unexpectedly and in contrast to PTEOS, that PTMOS is not fully hydrolyzed. The chemical

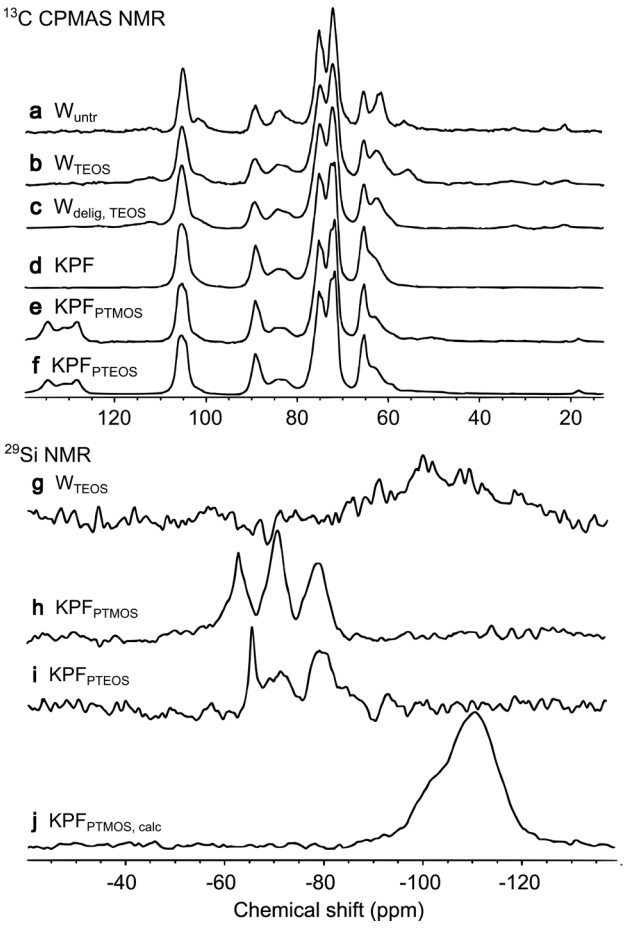

Figure 3 ^{13}C CPMAS NMR of (a) untreated and (b) TEOS-treated and (c) delignified and TEOS-treated pine wood pieces and (d) pulped and (e) PTMOS- and (f) PTEOS-treated KPF. ^{29}Si NMR spectra of (g) TEOS-treated pieces and (h) PTMOS-, (i) PTEOS-, and (j) PTMOS-treated and calcined fibers.

shift found at 18 ppm is assigned to EtOH and most likely due to small amounts of retained solvent. Both KPF_{PTMOS} and KPF_{PTEOS} (Figure 3e and f) display pronounced signals from phenyl groups between 125 and 135 ppm, confirming their inclusion in the treated wood (Brindle et al. 1995).

From ^{29}Si NMR analyses, the bonding states of the silicon atoms in the composites were determined (Figure 3b). In W_{TEOS} (Figure 3g), a low signal-to-noise ratio is indicative of the relatively small number of incorporated silicon atoms. However, the broad intensity distribution from ~90 to ~120 ppm is typical for the expected bonding states of tetraalkoxides of Q_0^2, Q_0^3, and Q_0^4 at -92, -102, and -112 ppm (Figure 1), respectively (Assink and Kay 1993; Sanchez et al. 1996). In the case of W_{PTMOS} (Figure 3h) and W_{PTEOS} (Figure 3i), the three bonding states T_0^1, T_0^2, and T_0^3 were found at -65, -71, and -78 ppm (Brindle et al. 1995; Jermouni et al. 1995). These shifts are higher than those reported for nonaromatic alkyl-substituted siloxanes (Salon et al.

2007) and are in agreement with data of Kuniyoshi et al. (2006) and Sun et al. (2006). Although there is no indication of a chemical shift due to silyl etherification (Liepiņš et al. 1986), this does not exclude the occurrence of such bonding. First, the number of precursors bonded to wood hydroxyl groups is expected to be low compared with the total amount of precursor. Second, there are no unambiguous data on the chemical shift of silicon alkoxides bound to wood hydroxyl groups (Tingaut et al. 2006). The T^1 peak of KPF_{PTMOS} fibers is at a higher chemical shift than that of KPF_{PTEOS} and than expected from the literature. The interpretation is that it is in fact a T_1^1 peak of a single OMe group from retained precursor molecules. This is most likely due to the residual OMe groups already found by ^{13}C NMR, which would cause a shift of the ^{29}Si NMR signal (Liepiņš et al. 1986; Jermouni et al. 1995; Alam and Henry 2000). Expectedly, after calcination of the treated samples (Figure 3j), only highly crosslinked Q^3 and Q^4 silicon species are present. It could be shown that the siloxane precursors are in a fully hydrolyzed but incompletely condensed state after the treatment. This may lead to reactive bonding in future applications as WPC materials.

Bonding states II: EIS

To determine the bonding states of the wood hydroxyl groups, EIS of treated fibers was employed. The measured dielectric losses ε_r'' were plotted against the permittivities ε_r', giving rise to the depressed semicircles in Figure 4. The measurement frequency range is particularly suited to detect changes in dipole oscillation processes due to C6 carbon-bonded hydroxyl groups in wood (Einfeldt et al. 2001). From data fitted according to Equation (1), several characteristic parameters of the dielectric spectra were calculated (Table 4).

$\varepsilon_{r\,max}''$ is the maximum dielectric loss and a qualitative measure of the total number of oscillators in the sample (Cole and Cole 1941). As expected, the samples show an $\varepsilon_{r\,max}''$ progression from KPF_{untr}>KPF_{TEOS}>KPF_{PTEOS}>KPF_{PTMOS}, which is in good agreement with the reduction of EMC (Seidman and Mason 1954; Ishida et al. 1959; Norimoto 1976; Jinzhen and Guangjie 2002; Sugiyama and Norimoto 2006). Considering their higher EMC, a stronger decrease of $\varepsilon_{r\,max}''$ could be expected in the KPF_{untr} during drying. However, $\varepsilon_{r\,max}''$ was disproportionately lowered by drying in KPF_{tr}, even when taking into account their lower wood content per mass. This is an indication of precursor bonding to wood, which lowers the amount of hydroxyl oscillators. The increased $\varepsilon_{r\,max}''$ for the KPF_{PTMOS} is interpreted as a sign of an additional relaxation process, as discussed in the following. In our measurements, the oscillator dipole moment distribution parameters (ε_0-ε_∞) found for KPF_{untr} and KPF_{tr} are in good agreement with literature data and do not change significantly during drying due to the overall low moisture contents (Ishida

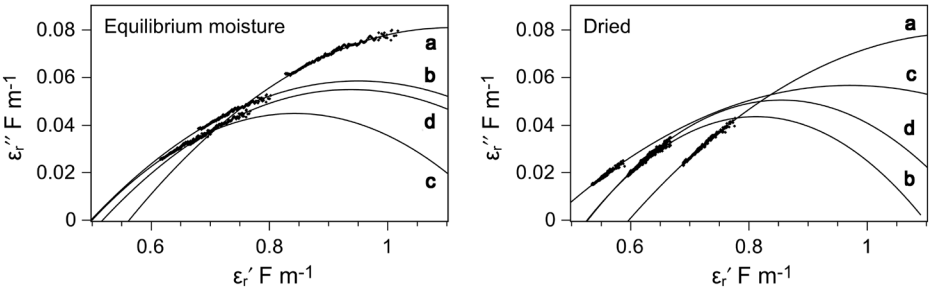

Figure 4 Sections of EIS Cole-Cole plots, with 800 measured frequencies each, from fibers at EMC and dried at 105°C. (a) Untreated and (b) TEOS-, (c) PTMOS-, and (d) PTEOS-treated KPF with fitted circular plots.

Table 4 Maximum dielectric loss $\varepsilon_{r\,max}''$, Cole-Cole parameters ε_0-ε_∞, β, and generalized relaxation times τ_0 determined by impedance measurements of untreated and TEOS-, PTMOS-, and PTEOS-treated KPF at EMC and dried at 105°C.

Sample	EMC				Dried			
	$\varepsilon_{r\,max}''$ F m^{-1}	ε_0-ε_∞ F m^{-1}	β (rad)	log(τ_0) (τ_0 in s)	$\varepsilon_{r\,max,dry}''$ F m^{-1}	ε_0-$\varepsilon_{\infty\,dry}$ F m^{-1}	β_{dry} (rad)	log($\tau_{0,dry}$) (τ_0 in s)
KPF_{untr}	0.081	1.085	0.223	-7.82	0.079	1.138	0.216	-5.16
KPF_{TEOS}	0.059	0.905	0.193	-6.93	0.044	0.572	0.254	-8.31
KPF_{PTMOS}	0.045	0.687	0.203	-6.60	0.057	1.014	0.179	-5.74
KPF_{PTEOS}	0.055	0.839	0.200	-6.61	0.051	0.655	0.245	-6.25

et al. 1959; Zhao et al. 1990; Sugimoto et al. 2005; Sugiyama and Norimoto 2006). They are generally lower in treated samples, supporting the hypothesis that the incorporated phases are indeed bound to hydroxyl groups of wood, as proposed by some authors (Donath et al. 2004; Tingaut et al. 2006). This means that the hydrophobic properties of the composites are in part due to the reaction of the hydroxyl groups by condensation with the siloxane precursor phase. Unexpectedly, $(\varepsilon_0\text{-}\varepsilon_\infty)$ increased in KPF_{PTMOS} dried at 105°C, which was attributed to the same relaxation process already shown by the increase of $\varepsilon''_{r\,max}$. The parameter β in Equation (4) is a measure of the range of relaxation times and therefore the range of molecules that participate in relaxation processes (Sugiyama and Norimoto 2006). In KPF_{untr}, the β values are in agreement with literature data and did not alter with the small moisture change during drying (Norimoto and Yamada 1972). In all KPF_{tr}, β was consistently lower than in KPF_{untr}, indicating a broader distribution of relaxation times due to water adsorbed on the incorporated material at different chemical surroundings (Fu and Zhao 2007). After drying, the reverse was true. This points to the removal of relaxation processes from precursor-bound water and possibly from particular species of wood hydroxyl groups. The quantitative contribution of the silanol groups from incompletely condensed precursors to the relaxation time broadening is unknown but qualitatively decreases β after drying. The narrowing of the relaxation time distribution by drying would therefore be even stronger if the silanol contribution were omitted, strongly indicating the reduction of wood hydroxyl movement in the treated samples. The generalized relaxation time τ_0 gives further insight into the species involved (Wagner 1913). Relaxation times reported in literature diverge significantly. Although our calculated τ_0 roughly agree with those found by Fu and Zhao (2007) and those expected from wood hydroxyl groups (Einfeldt et al. 2001), they are shorter by one order of magnitude than reported by Sugiyama and Norimoto (2006). The τ_0 were increased by the treatment with TEOS and even more by the treatment with PTMOS and PTEOS, most likely due to the bonding of the precursors to the wood C6 hydroxyl groups, removing the fast methylol contribution to the generalised relaxation time (Einfeldt et al. 2000, 2001; Sugiyama and Norimoto 2006). The reason for the reduction of τ_0 in the dried TEOS-treated fibers could not be clarified in this study. The conclusion is therefore that the hydrophobic behavior of the wood composites is due to a combination of pore filling, the inclusion of hydrophobic phenyl groups, and the etherification of cell-wall hydroxyl groups.

Thermal properties of the composites

The ash contents obtained from the KPF_{tr}, as shown in Table 3, are, due to the high porosity of fibers, consistently higher than in W_{tr}. They are very close to those found in $W_{delig,\,tr}$ indicating a similar accessibility of the fiber cell walls in both sample types. The difference between the WPGs and the ash contents of KPF_{PTMOS} and KPF_{PTEOS} matches the expected mass loss from the combustion of the phenyl groups, which make up 56% of an assumed completely condensed phenyl-substituted precursor molecule. The ash of KPF_{PTMOS} was lower than expected from the WPGs, indicating the presence of nonhydrolyzed and uncondensed precursor in the samples, even after several days of drying at 105°C. The boiling points (and heats of vaporization) of the precursors are based on DSC analysis: TEOS 145°C (469.05 J g^{-1}), PTMOS 175°C (597.2 J g^{-1}), and PTEOS 227°C (965.0 J g^{-1}). This means that uncondensed TEOS is removed from the wood during drying at a higher rate than PTMOS and particularly PTEOS. Tetraalkoxysilanes with shorter alkyl groups were found to hydrolyze more rapidly (Bernards et al. 1991). This entails a shorter hydrolysis time of PTMOS compared with PTEOS. Another advantage of PTMOS in this context should be the higher vapor pressure of methanol compared with EtOH, leading to a faster removal of condensation products, further accelerating the reaction. However, in our work, there were strong indications for the permanent presence of unhydrolyzed methoxy groups in the PTMOS-treated fibers. It can be assumed that there is a mechanism that decelerates the hydrolysis of the last alkoxy group in PTMOS more strongly than in other alkoxides. Tests with drying temperatures of 90°C and 105°C to maximize the reaction between wood hydroxyl groups and the precursors (Castellano and Gandini 2004) led to WPGs that were reduced by ~50% compared with those obtained at 50°C, 75°C, and 105°C. The thermal analyses of the treated products (Figure 5) showed that the residual masses at 800°C increase from TEOS (6%) over PTEOS (11%) to PTMOS (20%), as expected from their different crosslinking behavior and in agreement with the ash determinations.

The first and second exothermic mass loss steps, assigned to degradation and combustion of organic and carbon species (Beall 1971), are shifted to higher temperatures in the order KPF_{PTMOS}>KPF_{PTEOS}>KPF_{TEOS}>KPF_{untr}, showing the higher thermal stability of the modified products. The thermal behavior of the treated fibers is similar to that reported for phosphate and borate-modified wood (Miyafuji et al. 1998). The carbonization and combustion temperatures are higher than those of pure

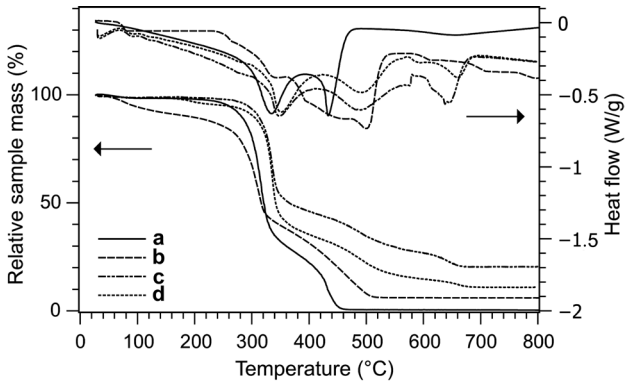

Figure 5 Combined TGA-DTA mass loss and heat flow curves of (a) untreated and (b) TEOS-, (c) PTMOS-, and (d) PTEOS-treated KPF. Negative heat flow indicates an exothermic process.

wood-inorganic composites (Saka and Ueno 1997). The composites W_{PTMOS} and W_{PTEOS} show a third exothermic mass loss at 650°C, which indicates the presence of a heat-resistant carbon species. Fourier transform infrared spectroscopy of samples heated up to 500°C at 8°C min^{-1} (data not shown), held for 5 min, and then immediately taken from the furnace showed the characteristic vibrational bands of phenyl rings at 2848, 1594, and 1428 cm^{-1}, indicating the presence of incorporated phenyl groups (Rao et al. 2003). These are mesomerically stabilized and thermally resistant (Johns et al. 1962). In TEOS-treated samples, the mass loss of 15% below 250°C is assigned to the evaporation of water, EtOH, and uncondensed TEOS, explaining the low ash contents obtained by monomeric TEOS treatment. The inclusion of stable phenyl rings is therefore the reason for the composites' higher temperature resistances.

Conclusion

By treating wood and wood fibers with PTMOS and PTEOS, organically modified siloxane-wood composite materials were obtained in a simple one-step impregnation process. The results can be safely interpreted as showing chemical bonding of the condensed precursors to the wood hydroxyl groups, most likely to the methylol groups. The composites are highly hydrophobic and resistant to water uptake due to the filling of cell wall micropores, the incorporation of hydrophobic phenyl groups, and the reaction of the precursors with hydrophilic hydroxyl groups. Due to this reactive bonding, the hybrid phase could not be leached. These properties are promising in terms of the application of PTMOS and PTEOS for effective bulk treatment of wood exposed to strong weathering and abrasion. The prepared wood fibers are highly lipophilic and the condensation state of the embedded precursors after drying is incomplete. Thus, the pretreated fibers are well suited as reactive fillers in WPC materials. The systematic testing of the influence of different WPGs on the properties of the composites will be studied in further research.

Acknowledgments: This work was performed as part of Project IX "Hierarchically structured porous ceramics and composites from nanocasting of plant cell walls" in the framework of the priority programme SPP1420 of the Deutsche Forschungsgemeinschaft (German Research Foundation). The grant of our project and the financial aid allocated to our work through SPP1420 is gratefully acknowledged.

Received January 15, 2013; accepted March 15, 2013; Previously published online April 11, 2013

References

Aaserud, J., Larnøy, E., Glomm, W. Alternative systems for wood preservation, based on treatment with silanes. In: Proceedings of the 5th meeting of the Nordic-Baltic Network in Wood Material Science and Engineering (WSE), October 1-2, 2009, Copenhagen, Denmark, 2009.

Alam, T., Henry, M. (2000) Empirical calculations of ^{29}Si NMR chemical shielding tensors: a partial charge model investigation of hydrolysis in organically modified alkoxy silanes. Phys. Chem. Chem. Phys. 2:23–28.

Allan, G.G., Carroll, J.P., Negri, A.R., Raghuraman, M., Ritzenhtaler, P., Yahiaoui, A. (1992) The microporosity of pulp: the precipitation of inorganic fillers within the micropores of the cell wall. Tappi 75:175–178.

Assink, R.A., Kay, B.D. (1993) The chemical kinetics of silicate sol-gels: functional group kinetics of tetraethoxysilane. Coll. Surf. A 74:1–5.

Attard, P., Antelmi, D., Larson, I. (2000) Comparison of the zeta potential with the diffuse layer potential from charge titration. Langmuir 16:1542–1552.

Beall, F.C. (1971) Differential calometric analysis of wood and wood components. Wood Sci. Technol. 5:159–175.

Bernards, T.N.M., Van Bommel, M.J., Boonstra, A.H. (1991) Hydrolysis-condensation processes of the tetra-alkoxysilanes TPOS, TEOS and TMOS in some alcoholic solvents. J. Non-Cryst. Sol. 134:1–13.

Brindle, R., Albert, K., Morgan, E.D., Martin, P., Wilson, I.D. (1995) Solid state NMR and extraction studies on "phenyl"-bonded stationary phases used for solid phase extraction. J. Pharm. Biomed. Anal. 13:1305–1312.

Brinker, C.J., Scherer, G.W. Sol-gel science. Academic Press, London, 1990.

Brunet, F. (1998) Polymerization reactions in methyltriethoxysilane studied through ^{29}Si NMR with polarization transfer. J. Non-Cryst. Sol. 231:58–77.

Burgert, I., Eder, M., Gierlinger, N., Fratzl, P. (2007) Tensile and compressive stresses in tracheids are induced by swelling based on geometrical constraints of the wood cell. Planta 226:981–987.

Castellano, M., Gandini, A. (2004) Modification of cellulose fibres with organosilanes: under what conditions does coupling occur? J. Coll. Interf. Sci. 273:505–511.

Cole, K.S., Cole, R.H. (1941) Dispersion and absorption in dielectrics I. Alternating current characteristics. J. Chem. Phys. 9:341–351.

Cookson, L.J., Scown, D.K., McCarthy, K.J., Chew, N. (2007) The effectiveness of silica treatments against wood-boring invertebrates. Holzforschung 61:326–332.

Donath, S., Militz, H., Mai, C. (2004) Wood modification with alkoxysilanes. Wood Sci. Technol. 38:555–566.

Einfeldt, J., Kwasniewski, A., Klemm, D., Dicke, R., Einfeldt, L. (2000) Analysis of side group motion in O-acetyl-starch using regioselective 2-O-acetyl-starches by means of dielectric spectroscopy. Polymer 41:9273–9281.

Einfeldt, J., Meißner, D., Kwasniewski, A. (2001) Polymerdynamics of cellulose and other polysaccharides in solid state-secondary dielectric relaxation processes. Prog. Polym. Sci. 26:1419–1472.

Elvy, S., Dennis, G., Ng, L. (1995) Effects of coupling agent on the physical properties of wood-polymer composites. J. Mater. Proc. Technol. 35:3417–3419.

Engelund, E.E.T., Thygesen, L.L.G., Svensson, S., Hill, C.A.S. (2013) A critical discussion of the physics of wood-water interactions. Wood Sci. Technol. 47:141–161.

Fahlén, J., Salmén, L., Fahlen, J., Salmen, L. (2005) Pore and matrix distribution in the fiber wall revealed by atomic force microscopy and image analysis. Biomacromolecules 6:433–438.

Fritz-Popovski, G., Opdenbosch, D., Zollfrank, C., Aichmayer, B., Paris, O., Van Opdenbosch, D. (2013) Development of the fibrillar and microfibrillar structure during biomimetic mineralization of wood. Adv. Funct. Mater. 23:1265–1272.

Fu, Y., Zhao, G. (2007) Dielectric properties of silicon dioxide/wood composite. Wood Sci. Technol. 41:511–522.

Hook, R. (1996) A ^{29}Si NMR study of the sol-gel polymerisation rates of substituted ethoxysilanes. J. Non-Cryst. Sol. 195:1–15.

Ishida, Y., Yōshino, M., Takayanagi, M., Irie, F. (1959) Dielectric studies on cellulose fibers. J. Appl. Polym. Sci. 1:227–235.

Jacobasch, H., Bauböck, G., Schurz, J. (1985) Problems and results of zeta-potential measurements on fibers. Coll. Polym. Sci. 24:3–24.

Jermouni, T., Smaihi, M., Hovnanian, N. (1995) Hydrolysis and initial polycondensation of phenyltrimethoxysilane and diphenyldimethoxysilane. J. Mater. Chem. 5:1203–1208.

Jinzhen, C., Guangjie, Z. (2002) Dielectric relaxation based on adsorbed water in wood cell wall under non-equilibrium state. Part 3. Desorption. Holzforschung 56:655–662.

Jitianu, A., Britchi, A., Deleanu, C., Badescu, V., Zaharescu, M. (2003) Comparative study of the sol-gel processes starting with different substituted Si-alkoxides. J. Non-Cryst. Sol. 319:263–279.

Johns, I.B., McElhill, E.A., Smith, J.O. (1962) Thermal stability of some organic compounds. J. Chem. Eng. Data 7:277–281.

Kirkwood, J.G., Fuoss, R.M. (1941) Anomalous dispersion and dielectric loss in polar polymers. J. Chem. Phys. 9:329–340.

Kuniyoshi, M., Takahashi, M., Tokuda, Y., Yoko, T. (2006) Hydrolysis and polycondensation of acid-catalyzed phenyltriethoxysilane (PhTES). J. Sol-Gel Sci. Technol. 39:175–183.

Liepiņš, E., Zicmane, I., Lukevics, E. (1986) A multinuclear NMR spectroscopy study of alkoxysilanes. J. Organomet. Chem. 306:167–182.

Loos, W. (1968) Dimensional stability of wood-plastic combinations to moisture changes. Wood Sci. Technol. 2:308–312.

Mahltig, B., Swaboda, C., Roessler, A., Böttcher, H. (2008) Functionalising wood by nanosol application. J. Mater. Chem. 18:3180–3192.

Mao, J., Holtman, K.M., Scott, J.T., Kadla, J.F., Schmidt-Rohr, K. (2006) Differences between lignin in unprocessed wood, milled wood, mutant wood, and extracted lignin detected by ^{13}C solid-state NMR. J. Agric. Food Chem. 54:9677–9686.

Miyafuji, B.H., Saka, S., Yamamoto, A., Miyafuji, H. (1998) Wood-inorganic composites prepared by metal alkoxide oligomers and their fire-resisting properties. Holzforschung 52:410–416.

Miyafuji, H., Kokaji, H., Saka, S. (2004) Photostable wood-inorganic composites prepared by the sol-gel process with UV absorbent. J. Wood Sci. 50:130–135.

Mohammed-Ziegler, I., Tanczos, I., Horvolgyi, Z., Agoston, B. (2008) Water-repellent acylated and silylated wood samples and their surface analytical characterization. Coll. Surf. A 319:204–212.

Norimoto, M. (1976) Dielectric properties of wood. Wood Res. 59:106–152.

Norimoto, M., Yamada, T. (1972) The dielectric properties of wood VI: on the dielectric properties of the chemical constituents of wood and the dielectric anisotropy of wood. Wood Res. Bull. Wood Res. Inst. Kyoto Univ. 52:31–43.

Pickering, K., Abdalla, A., Ji, C. (2003) The effect of silane coupling agents on radiata pine fibre for use in thermoplastic matrix composites. Compos. A 34:915–926.

Podgorski, L., Chevet, B., Onic, L., Merlin, A. (2000) Modification of wood wettability by plasma and corona treatments. Int. J. Adhes. Adhes. 20:103–111.

Pétrissans, M., Gérardin, P., Serraj, M. (2003) Wettability of heat-treated wood. Holzforschung 57:301–307.

Rao, A.V., Kalesh, R.R., Pajonk, G.M. (2003) Hydrophobicity and physical properties of TEOS based silica aerogels using phenyltriethoxysilane as a synthesis component. J. Mater. Sci. 8:4407–4413.

Rowell, R., Ellis, W. (1978) Determination of dimensional stabilization of wood using the water-soak method. Wood Fiber Sci. 10:104–111.

Rowell, R.M., Gutzmer, D., Sachs, I., Kinney, R. (1976) Effects of alkylene oxide treatments on dimensional stability of wood. Wood Sci. 9:14–194.

Rozman, H.D., Kumar, R.N., Abusamah, A. (1995) Rubberwood-polymer composites based on diallyl phthalate and methyl methacrylate. J. Appl. Polym. Sci. 57:1291–1297.

Rösch, L., John, P., Reitmeier, R. (2000) Silicon compounds, organic. In: Ullmann's Encyclopedia of Industrial Chemistry. Wiley-VCH, Weinheim. pp. 637–674.

Saka, S., Ueno, T. (1997) Several SiO_2 wood-inorganic composites and their fire-resisting properties. Wood Sci. Technol. 31:457–466.

Saka, S., Sasaki, M., Tanahashi, M. (1992) Wood-inorganic composites prepared by sol-gel processing. I. Wood-inorganic composites with porous structure. Mokuzai Gakkaishi 38:1043–1049.

Salon, M.-C.B., Gerbaud, G., Abdelmouleh, M., Bruzzese, C., Boufi, S., Belgacem, M.N. (2007) Studies of interactions between silane coupling agents and cellulose fibers with liquid and solid-state NMR. Magn. Reson. Chem. 45:473–483.

Sanchez, J., Rankin, S.E., McCormick, A.V. (1996) ^{29}Si NMR kinetic study of tetraethoxysilane and ethyl-substituted ethoxysilane polymerization in acidic conditions. Ind. Eng. Chem. Res. 35:117–129.

Seidman, R., Mason, S.G. (1954) Dielectric relaxation in cellulose containing sorbed vapors. Can. J. Chem. 32:744–762.

Stamm, A.A.J., Hansen, L., Seborg, R.M. (1936) Minimizing wood shrinkage and swelling. Ind. Eng. Chem. 28:1164–1169.

Stark, N.M., Matuana, L.M. (2007) Characterization of weathered wood–plastic composite surfaces using FTIR spectroscopy, contact angle, and XPS. Polym. Degrad. Stabil. 92:1883–1890.

Sugahara, Y., Inoue, T., Kuroda, K. (1997) ^{29}Si NMR study on co-hydrolysis processes in Si(OEt)4-RSi(OEt)3-EtOH-water-HCl systems (R=Me, Ph): effect of R-groups. J. Mater. Chem. 7:53–59.

Sugimoto, H., Takazawa, R., Norimoto, M. (2005) Dielectric relaxation due to heterogeneous structure in moist wood. J. Wood Sci. 51:549–553.

Sugiyama, M., Norimoto, M. (2006) Dielectric relaxation of water adsorbed on chemically treated woods. Holzforschung 60:549–557.

Sun, X., Xu, Y., Jiang, D., Yang, D., Wu, D., Sun, Y., Yang, Y., Yuan, H., Deng, F. (2006) Study on the ammonia-catalyzed hydrolysis kinetics of single phenyltriethoxysilane and mixed phenyltriethoxysilane/tetraethoxysilane systems by liquid-state ^{29}Si NMR. Coll. Surf. A 289:149–157.

Sèbe, G., De Jéso, B. (2000) The dimensional stabilisation of maritime pine sapwood (*Pinus pinaster*) by chemical reaction with organosilicon compounds. Holzforschung 54:474–480.

Tanno, B.F., Saka, S., Yamamoto, A., Takabe, K. (1998) Antimicrobial TMSAH-added wood-inorganic composites prepared by the sol-gel process. Holzforschung 52:365–370.

Taylor, C., Aloisio, C. (1985) Mechanical relaxation of flame retardant polycarbonate using the Cole-Cole method. Polym. Eng. Sci. 25:105–112.

Temiz, A., Terziev, N., Jacobsen, B., Eikenes, M. (2006) Weathering, water absorption, and durability of silicon, acetylated, and heat-treated wood. J. Appl. Polym. Sci. 102:4506–4513.

Tingaut, P., Weigenand, O., Mai, C., Militz, H., Sèbe, G. (2006) Chemical reaction of alkoxysilane molecules in wood modified with silanol groups. Holzforschung 60:271–277.

Tjeerdsma, B.F., Boonstra, M., Pizzi, A., Tekely, P., Militz, H. (1998) Characterisation of thermally modified wood: molecular reasons for wood performance improvement. Holz als Roh- und Werkstoff 56:149–153.

Unger, B., Bücker, M., Reinsch, S., Hübert, T. (2012) Chemical aspects of wood modification by sol-gel-derived silica. Wood Sci. Technol. 47:1–22.

Van Opdenbosch, D., Fritz-Popovski, G., Paris, O., Zollfrank, C. (2011) Silica replication of the hierarchical structure of wood with nanometer precision. J. Mater. Res. 26:1193–1202.

Wagner, K.K.W. (1913) Zur Theorie der unvollkommenen Dielektrika. Ann. Phys. 345:817–855.

Wu, Z., Xiang, H., Kim, T., Chun, M.-S., Lee, K. (2006) Surface properties of submicrometer silica spheres modified with aminopropyltriethoxysilane and phenyltriethoxysilane. J. Coll. Interf. Sci. 304:119–124.

Xie, Y., Hill, C.A.S., Xiao, Z., Militz, H., Mai, C. (2010) Silane coupling agents used for natural fiber/polymer composites: a review. Compos. A 41:806–819.

Zhao, G.J., Norimoto, M., Yamada, T., Morooka, T. (1990) Dielectric relaxation of water adsorbed on wood. Mokuzai Gakkaishi 36:257–263.